Int. J. Electrochem. Sci., 15 **(2020)** 4117 – 4126, doi: 10.20964/2020.05.25

International Journal of
ELECTROCHEMICAL
SCIENCE
www.electrochemsci.org

Electrochemical Corrosion Behavior of Ni-doped ZnO Thin Film Coated on Low Carbon Steel Substrate in 3.5% NaCl Solution

Duo Zhang, Mingming Wang, Nan Jiang[*]*, Yan Liu, Xiaonan Yu, Haobo Zhang,*

School of Mechanical Engineering, North China University of Science and Technology, Tangshan, China
[*]E-mail: jiangnansci@aliyun.com

Received: 1 January 2020 / *Accepted:* 23 February 2020 / *Published:* 10 April 2020

A facile sol-gel technique was successfully used to deposit Ni-doped ZnO thin film on low carbon steel substrates for evaluation of electrochemical corrosion resistance. The morphology, composition and crystalline phase of the coatings were obtained by scanning electron microscopy, energy dispersive X-ray spectroscopy, X-ray diffraction and atomic force microscopy. The evaluation of corrosion protection was carried out by potentiodynamic and electrochemical impedance spectroscopy analysis in 3.5% NaCl solution. The electrochemical results show that the uniform and thick coatings of Ni-doped ZnO thin film as an insulator indicated higher resistances and lower capacitances than other samples. The assessment of coating thickness influences on corrosion protection revealed that the sample with 454 nm thickness had a lower corrosion current density and higher corrosion potential than that of the other samples, indicating a better performance in corrosion resistance.

Keywords: Ni-doped ZnO; Corrosion resistance; Low carbon steel; Sol-gel technique; Electrochemical study

1. INTRODUCTION

Corrosion of steel is one of the problems that cause disastrous damage to steel structures and alloys which can lead to economic consequences such as replacement, product losses, repair, environmental pollution and safety [1, 2]. Therefore, further evaluation in this case is necessary to improve the performance of steel structures. Low carbon steel (LCS) is widely used materials which plays a major role in the metallurgical industry [3].

There are many methods to protect LCS from corrosion in harsh environments [4]. Among others, organic coatings are widely used to provide higher corrosion resistance for steel in the industry [5]. Recently, ceramic coatings as coating materials had attracted more attention due to their excellent

electrical and thermal properties [6, 7]. Furthermore, they show more resistant to corrosion, wear, oxidation and erosion than metals in aggressive and high temperature environments [8]. Thus, ceramic oxide thin films and coatings such as silica, titania, alumina and zinc oxide can be coated on steel to modify their surface properties [9-11].

Several techniques are employed to coat ceramic materials on steel surfaces such as laser cladding sol-gel process, plasma spraying and chemical vapor deposition [12]. Among all the accessible approaches, the sol-gel method seems to be the most appropriate. Sol-gel technique is a chemical procedure that prepares ceramic materials at low temperatures [13].

Electrochemical approaches have been broadly used by some researchers to investigate the corrosion behavior of coating materials [14]. Electrochemical impedance spectroscopy (EIS) method is an effective and compelling tool for the analysis of corrosion process of coated metals [15].

However, there is an extensive work to study the unique properties of ZnO and Ni nanostructures [16-18], no previous studies had reported a combination of both in protective coatings. Thus, in this study, Ni-doped ZnO coated on LCS substrate was prepared by sol-gel method. Furthermore, the electrochemical technique were used to evaluate the corrosion behavior of the samples and the effects of coating thickness on corrosion resistance.

2. MATERIALS AND METHOD

The preparation of precursor solutions were done by the sol–gel technique using nickel acetate and zinc acetate for both Ni-doped ZnO (NZO) and undoped ZnO. First, 0.8 g zinc acetate (as a precursor) was directly dissolved into 20 mL of ethanol to get a Zn stock solution (for coating undoped ZnO). Then, the 0.2 M nickel acetate was dissolved in methyl cellosolve under a nitrogen flow. The solutions was stirred and heated at 80 ℃ on the hot plate for 1 hour until it became clear and homogeneous. Then, the solution was sonicated at 50 ℃ for 1 hour by using an ultrasonic water bath. Finally, both the prepared solutions were blended to produce the stable, transparent, and stoichometric NZO precursor. The final solution (0.4 M concentration) was green colored and transparent. Before coating it on steel surface, the prepared solution was aged for one day. The AISI 1018 low carbon steel (LCS) coupons (10*10 mm^2) were polished by silicon carbide papers down to 2500# (LANHU, Germany), and finally all samples were cleaned in acetone in an ultrasonic cleaner (Mophorn, China) and washed in distilled water for 20 min. A dip-coating method was used to form ZnO and NZO on the LCS substrate at 0.5 mm/s withdrawal speed. Immediately after the coating process, the thin films were heated to 300 ℃ for 10 minutes to evaporate the solvent. The samples were then heat-treated for 1 hour at 450 ℃ to activate the oxide conversion and eliminate the residual and the organic contaminations.

Electrochemical analysis of the samples was carried out by electrochemical impedance spectroscopy (EIS) technique. A conventional three-electrode cell was applied for the measurements which contain the coated LCS substrate as working electrode, a platinum wire as a counter electrode and a saturated calomel electrode as the reference electrode with 3.5 wt% NaCl solution as working electrolyte. The EIS analysis was done in a frequency range of 0.01 Hz to 0.1 MHz. The

potentiodynamic polarization (CorrTest Instruments Corp., Ltd., China) measurement was performed at 1 mV/s scanning rate from 0 V to -0.7 V. The morphology of the Ni-doped ZnO (NZO)/ low carbon steel (LCS) substrate was analyzed by scanning electron microscopy (SEM, FEI Sirion 200). The surface topography of NZO/LCS substrate was performed by atomic force microscopy (Veeco Instruments, Inc., USA, AFM) with an operation of contact mode. Crystallinity analysis of ZnO and NZO coated LCS was performed with Xpert Pro X-ray diffractometer with 1.5404 Å (Cu Kα) in wavelength and 40KV/30 mA in power.

3. RESULTS AND DISCUSSION

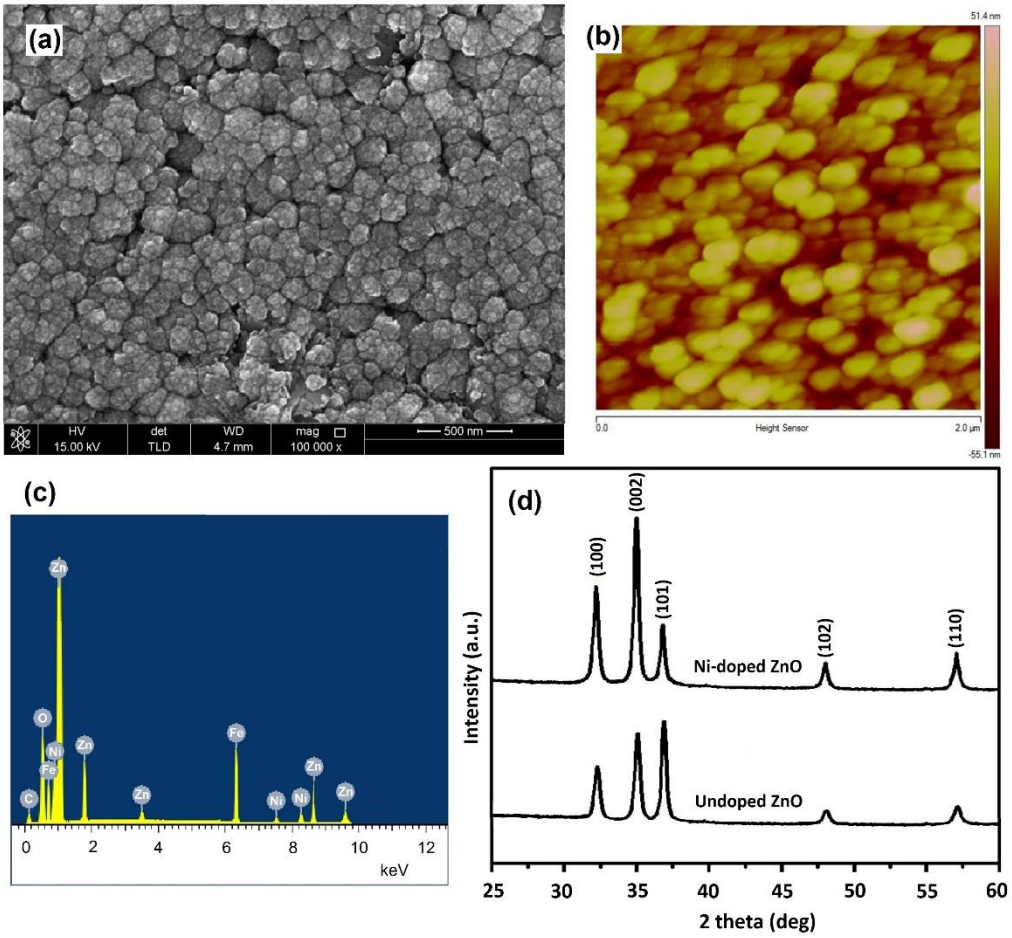

Figure 1. (a) FESEM, (b) AFM images and (c) EDX analysis of NZO thin film and (d) XRD pattern of the bare and NZO films.

The surface morphology of Ni-doped thin films was observed by SEM image in Figure 1a. As shown, the sample have smooth surface including well faceted grains.

In order to study on the surface roughness of the Ni-doped ZnO (NZO) thin film, the AFM was done. Figure 1b indicates the AFM image of NZO thin film formed on low carbon steel (LCS) substrate. The average roughness of the NZO thin films was 33.5 nm. The high value of surface roughness in NZO thin film might be due to the improvement in the amount of nucleation sites

through Ni dopants [19, 20]. Figure 1c shows the EDX results of the sample which proved the presence of nickel, oxygen and zinc in the NZO film. The presence of Fe and C in the film can be attributed to the substrate effect to eliminate charging effects.

Figure 1d shows the XRD pattern of the bare and NZO films. It confirms that the deposited thin films were polycrystalline with hexagonal wurtzite structures which were corresponding with JCPDS card (36-1451) [21]. Furthermore, no peaks related to NiO or Ni appeared in the doped thin film which had proven the solubility limit of NZO film. The increasing intensity of the peaks and reduction of peak width proposed that the quality of the crystal structure in the NZO film was enhanced by Ni-doping. The lattice parameter for (0 0 2) plane in the undoped and NZO were 5.1127 Å and 5.1158 Å, respectively. The larger lattice constant of NZO proved that the Ni ions are existent in the ZnO interstitial sites.

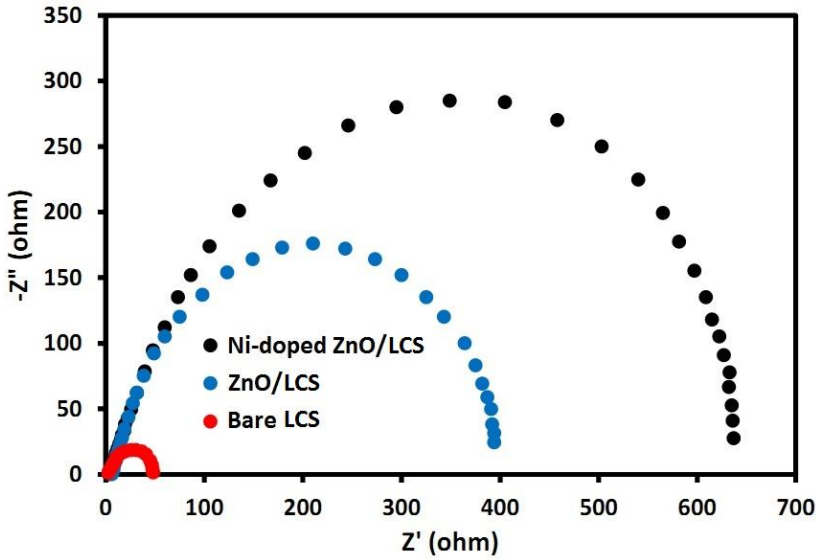

Figure 2. The Nyquist plots of bare LCS, undoped and NZO coating on LCS substrates in 3.5% NaCl solution.

The EIS was used to evaluate the corrosion behavior of ZnO thin films doped with Ni on LCS in 3.5% NaCl solution. The Nyquist plots for bare LCS, and undoped and NZO coating on LCS substrates in 3.5% NaCl solution in figure 2. The overall shape of the plots was the same for all specimens, with only single capacitive semicircle appearing for each sample. A great capacitive loop was found for the NZO coated specimen which was larger than the bare LCS and ZnO coated LCS substrates. The capacitive loop is apparently related to the EIS results of the corrosion process happening at the NZO coated steel interface [22]. The existence of only one semicircle in the Nyquist diagrams show that the corrosion of NZO coatings contain a single time constant. Therefore, it is obvious that the NZO coatings in the aggressive media interface reveal the mechanism of charge transfer. The EIS results was attained by equivalent circuit and experimental fitted data. The equivalent circuit model used is indicated in Fig. 3.

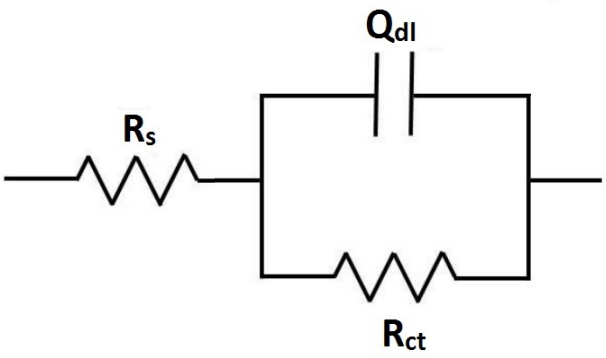

Figure 3. An equivalent circuit model

Where R_s is the resistance of solution [23]. R_{ct} and Q_{dl} are charge transfer resistance in steel surface and constant phase element, respectively [24]. In this equivalent circuit, the constant phase element was used for a double-layer capacitance due to the non-ideal property of the response. It is because of the coating materials which had resulted in a certain surface roughness and homogeneities. Mahmoudian et al. suggested the same equivalent electrical circuit to consider the behavior of polypyrrole/TiO2 nanostructure coatings on mild steel at 3.5 wt% NaCl solution [25]. The determined data are indicated in Table 1.

Table 1. The attained data of fitting the Nyquist diagrams for samples with different coating.

Samples	R_s (Ω)	R_{ct} (Ω cm^2)	Q_{dl}(µF cm^{-2})
LCS	5.3	48	0.34
ZnO/LCS	6.7	406	0.17
Ni-doped ZnO/LCS	8.8	645	0.12

As shown in table 1, the R_{ct} values of LCS, ZnO/LCS and Ni-doped ZnO/LCS samples were 48, 406 and 645 Ωcm^2, respectively. The calculated Q_{dl} were 0.34, 0.17 and 0.12 µF cm^{-2} for LCS, ZnO/LCS and Ni-doped ZnO/LCS samples, respectively. The Ni-doped ZnO/LCS sample had the lowest Q_{dl} and the highest R_{ct}, which indicates reduced electrolyte access to the LCS substrate due to compact structure of the coating materials. The highest R_{ct} value of LCS substrate coated with NZO layer shows the best barrier feature indicating an increase in corrosion resistance ability. Furthermore, reducing Q_{dl} by increasing the coating thickness increases corrosion resistance [26, 27]. Moreover, the decrease in Q_{dl} value can be related to a reduction in the local dielectric constant. Enhanced performance in corrosion experiments indicated that adding nickel ions to the ZnO nanostructure had resulted in significant synergies and increased the protection of low carbon steel.

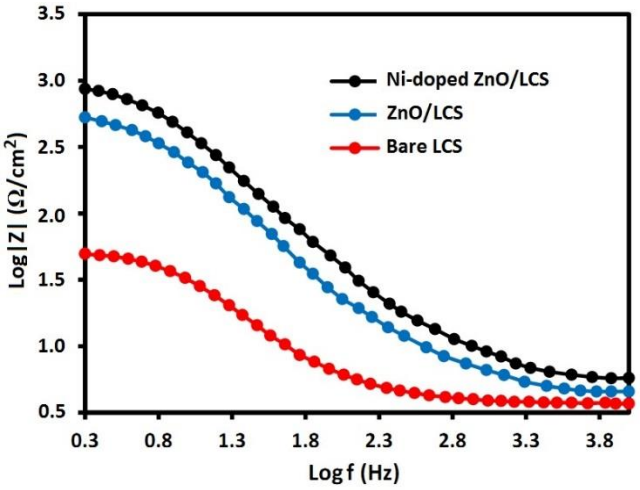

Figure 4. Bode plots of bare LCS, undoped and NZO coating on LCS substrates

The Bode diagrams attained from the EIS results are revealed in Fig. 4. Figure 4 shows that Ni-doped ZnO/LCS sample indicates the best performance to inhibit the corrosion behavior in marine environment. Furthermore, the diagrams of all specimens indicate one time constants showing that, a uniform and dense coating on the LCS.

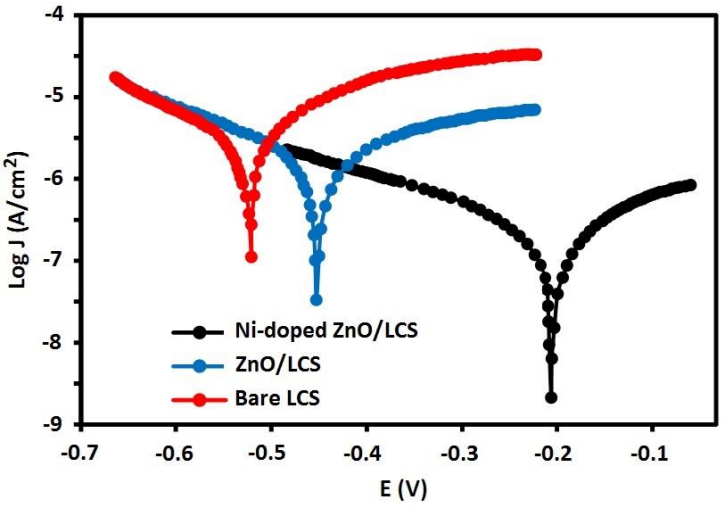

Figure 5. Potentiodynamic polarization of samples in 3.5 wt% NaCl solution after 20 hours exposure time

The corrosion resistance of the samples can be evaluated by polarization plots. Figure 5 shows polarization plots of LCS substrate with different coating materials exposed to 3.5 wt% NaCl solution after 20 hours exposure time. Clearly, the coating materials can provide separation of the LCS substrate with a corrosive medium. As shown in fig. 5, the anodic polarization plots are investigated by passive zones for all samples, showing that the passive layers had clearly formed on the surface of steel once they were exposed to the marine environment [28]. Moreover, a significant shift was observed in corrosion potential to a positive direction which revealed that the dissolution of anodic metal was effectively retarded by the coating materials [29]. The values of corrosion current density

(I_{corr}) and corrosion potential (E_{corr}) are indicated in table 2 which are taken from the polarization diagrams in Figure 5.

Generally, a higher E_{corr} and a lower I_{corr} indicate a better corrosion resistance [30]. As shown, the I_{corr} reduced from 6.3×10^{-6} A·cm^{-2} to 0.3×10^{-6} A·cm^{-2} which can be attributed to the thicker and compact coating materials that most corrosion reactions formed on the solution/coating interface.

Table 2. Corrosion current density and potential of the bare LCS, undoped and NZO coating on LCS substrates

Samples	Corrosion current density	Corrosion potential
Bare LCS	6.3 µA/cm^2	-0.521 V
ZnO/LCS	1.6 µA/cm^2	-0.443 V
Ni-doped ZnO/LCS	0.3 µA/cm^2	-0.216 V

As shown in Fig. 1a, the nanostructure can trap a large amount of air, so the air cushion can provide effective protection against Cl^- attack [31]. Moreover, the corrosive solution including Cl^- ions can be repulsed through Laplace pressure and the coated LCS substrate can be protected efficiently [32, 33]. These findings show that Ni-doped ZnO/LCS substrate has an outstanding corrosion resistance.

In order to study on the thickness effect of coating layer on corrosion behavior of LCS, potentiodynamic polarization test was done.

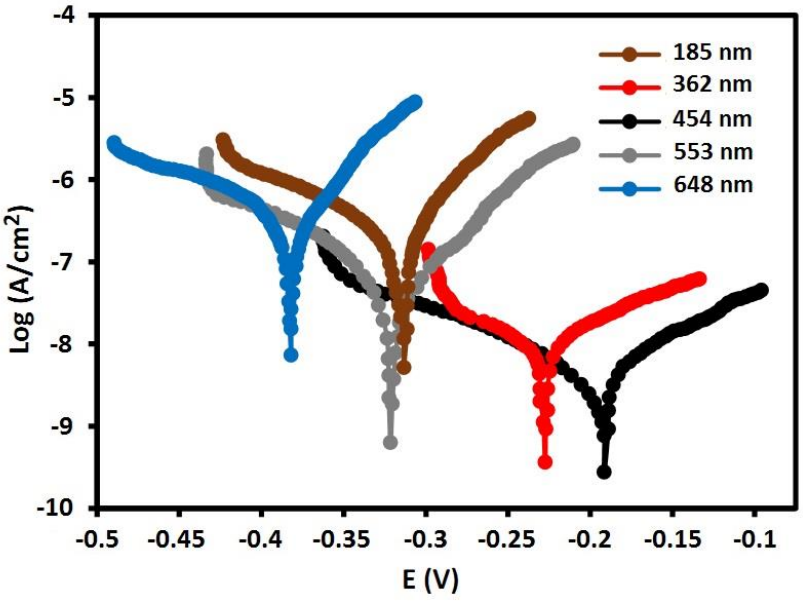

Figure 6. Potentiodynamic polarization plots of the specimens with various coating thickness in 3.5 wt% NaCl solution.

Fig. 6 indicates potentiodynamic polarization plots of samples with different coating thickness in 3.5 wt% NaCl solution. The Ni-doped ZnO/LCS substrate with 185, 362, 454, 553, and 648 nm

thickness were prepared 2, 3, 4, 5 and 6 times sol–gel coatings, respectively. The electrochemical parameters attained from potentiodynamic polarization plots are given in Table 3.

Table 3. The electrochemical parameters attained from potentiodynamic polarization plots of the samples

Coating thickness	Corrosion current density	Corrosion potential
185 nm	0.3 μA/cm^2	-0.316 V
362 nm	0.02 μA/cm^2	-0.225 V
454 nm	0.007 μA/cm^2	-0.185 V
553 nm	0.1 μA/cm^2	-0.322 V
648 nm	0.6 μA/cm^2	-0.382 V

As shown in table 3, the samples with the coating thickness of 185, 362 and 454 nm exhibit similar behavior against corrosion resistance. The decrease of I_{corr} and enhancement of E_{corr} can be observed by increasing the coating thickness. The sample with 454 nm thickness shows a lower I_{corr} than that of the other samples. The E_{corr} was shifted positively to -0.185 V. However, when the coating thickness was increased more, the cathodic shifts of the E_{corr} was found, indicating the reduction of corrosion protection performances. A similar electrochemical behavior was observed in Masalaki et al. research on corrosion resistance of Al_2O_3 coatings on 316L stainless steel in a corrosive environment [34]. The corrosion resistance reduction with increasing coating thickness over 454 nm can be attributed to the defection and adhesion of the coatings due to the stress produced in the film thickness because of the successive application of thermal and sol treatments. Furthermore, during the densification and crystallization procedure, and removal of residual organic and hydroxyl groups, cracks can be formed which cause the substrate to deform near the edges [35].

4. CONCLUSIONS

In this study, the NZO thin film coated on LCS substrates was prepared by dip-coating and sol-gel methods for investigation of LCS corrosion protection. The coating layer were considered in detail by SEM, AFM, XRD and EDX. The doping of ZnO with Ni had improved the surface area and led to a protection on the ZnO coating morphology. Structural measurements exhibited good Ni dispersion in ZnO matrix. The high corrosion resistance of LCS substrate gained by coating with NZO can be attributed to the low value of surface roughness and high compact of the film. The EIS results indicated that Ni-doped ZnO/LCS substrate had the lowest C_{dl} and the highest R_{ct}, introducing the excellent barrier property of the thin film. The evaluation of the influence of coating thickness on corrosion protection revealed that the sample with 454 nm thickness had a lower corrosion current density and higher corrosion potential than that of the other samples, indicating its better performance of corrosion resistance. The polarization results showed that the corrosion resistance of the coated LCS relates not only to the composition but also to its coating thickness.

ACKNOWLEDGEMENT
This work was supported by a research grant from the colleges and universities in Hebei province science and technology research youth fund (Grant No.QN2019076).

References

1. A. El-Meligi, *Journal of Empirical Research in Accounting & Auditing*, 3 (2016) 147.
2. K.Z. Sulay, A.U. Victor, B. Obed and A.O. Olufemi, *International Journal of Materials and Chemistry*, 5 (2015) 64.
3. H. Chen, S. Zhang, Z. Zhao, M. Liu and Q. Zhang, *Progress in Chemistry*, 31 (2019) 571.
4. D. Yuan, C. Zhang, S. Tang, X. Li, J. Tang, Y. Rao, Z. Wang and Q. Zhang, *Water research*, 163 (2019) 114861.
5. S. Tang, N. Li, D. Yuan, J. Tang, X. Li, C. Zhang and Y. Rao, *Chemosphere*, 234 (2019) 658.
6. D. Sidane, D. Chicot, S. Yala, S. Ziani, H. Khireddine, A. Iost and X. Decoopman, *Thin Solid Films*, 593 (2015) 71.
7. P. Shao, J. Tian, F. Yang, X. Duan, S. Gao, W. Shi, X. Luo, F. Cui, S. Luo and S. Wang, *Advanced Functional Materials*, 28 (2018) 1705295.
8. D. He, Y. Lei, C. Zhang, S. Li, X. Liu, H. Zhang, Q. Lv, Y. Wu and L. Jiang, *International Journal of Hydrogen Energy*, 40 (2015) 2899.
9. I. Santana, A. Pepe, E. Jimenez-Pique, S. Pellice, I. Milošev and S. Ceré, *Surface and Coatings Technology*, 265 (2015) 106.
10. R. Bernardie, S. Valette, J. Absi and P. Lefort, *Surface and Coatings Technology*, 276 (2015) 677.
11. P. Shao, J. Tian, X. Duan, Y. Yang, W. Shi, X. Luo, F. Cui, S. Luo and S. Wang, *Chemical Engineering Journal*, 359 (2019) 79.
12. X. He, F. Deng, T. Shen, L. Yang, D. Chen, J. Luo, X. Luo, X. Min and F. Wang, *Journal of colloid and interface science*, 539 (2019) 223.
13. E.-S. Ghaith, S. Hodgson and M. Sharp, *Journal of Materials Science: Materials in Medicine*, 26 (2015) 83.
14. J. Rouhi, S. Mahmud, S.D. Hutagalung and S. Kakooei, *Journal of Micro/Nanolithography, MEMS, and MOEMS*, 10 (2011) 043002.
15. F. Husairi, J. Rouhi, K. Eswar, A. Zainurul, M. Rusop and S. Abdullah, *Applied Physics A*, 116 (2014) 2119.
16. C.K. Sahoo and M. Masanta, *Journal of Materials Processing Technology*, 240 (2017) 126.
17. B. Ramezanzadeh and M. Attar, *Progress in Organic Coatings*, 71 (2011) 314.
18. N. Naderi, M. Hashim and J. Rouhi, *International Journal of Electrochemical Science*, 7 (2012) 8481.
19. S. Patil, S. Shinde and K. Rajpure, *Ceramics International*, 39 (2013) 3901.
20. J. Rouhi, C.R. Ooi, S. Mahmud and M.R. Mahmood, *Materials Letters*, 147 (2015) 34.
21. R. Dalvand, S. Mahmud and J. Rouhi, *Materials Letters*, 160 (2015) 444.
22. R. Antunes, M. De Oliveira and M. Pillis, *International Journal of Electrochemical Science*, 8 (2013) 1487.
23. K.M. Emran and H. AL-Refai, *International Journal of Electrochemical Science*, 12 (2017) 6404.
24. N. Naderi, M. Hashim, K. Saron and J. Rouhi, *Semiconductor Science and Technology*, 28 (2013) 025011.
25. M. Mahmoudian, Y. Alias, W. Basirun and M. Ebadi, *Applied Surface Science*, 268 (2013) 302.
26. W. Zhang, Z. Jiang, G. Li, Q. Jiang and J. Lian, *Surface and Coatings Technology*, 202 (2008) 2570.

27. P. Shao, X. Duan, J. Xu, J. Tian, W. Shi, S. Gao, M. Xu, F. Cui and S. Wang, *Journal of hazardous materials*, 322 (2017) 532.
28. R. Antunes, M. De Oliveira and I. Costa, *Materials and Corrosion*, 63 (2012) 586.
29. S. Kakooei, J. Rouhi, E. Mohammadpour, M. Alimanesh and A. Dehzangi, *Caspian Journal of Applied Sciences Research*, 1 (2012) 16.
30. W. Xu, J. Song, J. Sun, Y. Lu and Z. Yu, *ACS applied materials & interfaces*, 3 (2011) 4404.
31. S. Zheng, C. Li, Q. Fu, M. Li, W. Hu, Q. Wang, M. Du, X. Liu and Z. Chen, *Surface and Coatings Technology*, 276 (2015) 341.
32. T. Liu, S. Chen, S. Cheng, J. Tian, X. Chang and Y. Yin, *Electrochimica Acta*, 52 (2007) 8003.
33. P. Shao, L. Ding, J. Luo, Y. Luo, D. You, Q. Zhang and X. Luo, *ACS applied materials & interfaces*, 11 (2019) 29736.
34. J. Masalski, J. Gluszek, J. Zabrzeski, K. Nitsch and P. Gluszek, *Thin Solid Films*, 349 (1999) 186.
35. H. Cheraghi, M. Shahmiri and Z. Sadeghian, *Thin Solid Films*, 522 (2012) 289.